Optical Field Angle Distortion Calibration of FGS3

W. Jefferys[1], A. Whipple[1], Q. Wang[1], B. McArthur[1], G. F. Benedict[1], E. Nelan[1]
D. Story[1], and L. Abramowicz-Reed[2]

Abstract

The Hubble Space Telescope carries three Fine Guidance Sensors (FGS) that serve as part of the Pointing Control System and can be used for millisecond of arc astrometry on stars as faint as V=17. The *HST* Ritchey-Chrétien design produces optical distortions in the field of view of the telescope, which because of residual misalignments, must be calibrated on-orbit for any instrument. The method chosen to calibrate these distortions, as they are observed by the FGS, involves exploiting the metric invariance of a rich star cluster with respect to repointing the telescope; that is, the measured relative positions of stars, after calibration, should not depend on where the telescope was pointed. We report the analysis of an extensive series of measurements of the ecliptic open cluster M35, for the purpose of determining distortion polynomial coefficients and other parameters necessary to reduce *HST* astrometric observations with Fine Guidance Sensor 3. Implications for the accuracy of *HST* astrometry are discussed.

I. Introduction

The Hubble Space Telescope is a Cassegrain telescope of the Ritchey-Chrétien design. The prescription of the Optical Telescope Assembly (OTA) contains optical field angle distortion (OFAD) and some astigmatism. Neither coma nor spherical aberration was included in the optical design. The Fine Guidance Sensors (FGS) are optical interferometers that measure pointing changes by means of shearing the wavefront with Koester's prisms. (For details regarding the entire FGS design see Bradley et al. 1991.) Before light strikes the *HST* focal plane it is diverted to an FGS by means of a pick-off mirror. Next in the optical path is an aspheric mirror that corrects for the design astigmatism and almost totally collimates the beam. Following the asphere is a Star Selector composed of two fold flat mirrors and a five element corrector group which rotate as one unit. After the corrector group, the beam is totally collimated. Also, the pupil is located beyond this point (see Figure 1 in Bradley et al. 1991 for the optical layout of the FGS).

The combined OTA/FGS design contains distortion and lateral color effects. Distortion is a field dependent aberration that displaces the true star position but does not degrade image quality. The lateral color displaces the true star position as a function of field location and color temperature of the target. The design distortion

1. Astronomy Department and McDonald Observatory, University of Texas, Austin, Texas 78712
2. Hughes Danbury Optical Systems, Danbury, Connecticut 06810

within the FGS can impart pointing errors as large as 6 arc seconds. Lateral color contributes about 5 mas (worst case) to positional error. Although the design distortion is large, initial estimates for its signature are obtained through raytraces. Hence a substantial amount of design distortion can be removed with pre-launch estimates. Also, the majority of the design distortion results in an effect that mimics a change in the plate scale. The nonlinear distortion is only about 0.5 arc seconds.

The classical telescope design and lateral color are not the only sources of distortion that affect astrometric measurements. Figure errors on optical surfaces that are not near the pupil generate local wavefront tilts. The FGS pick-off, aspheric and Star Selector A fold mirrors are in this category. Figure error in the optical elements that are located beyond the five element corrector group of Star Selector A have no effect on the data, since the beam is totally collimated at that point. Misaligned Star Selector mirrors and clocking offsets between the Star Selectors and their respective encoders also contribute to distortion. Encoder bit errors add both low and high spatial frequency distortions to the target's location. Finally, launch stress, moisture desorption and misaligned optical elements will change the signature of design distortion. Astrometric data must be adjusted for these distortions. Prior to launch these contributors were identified and methods to remove their effects, via on-orbit calibrations or subtraction maps, were devised.

Of course, it is well known that the *HST* OTA design was not realized (Burrows et al., 1991). Due to figure error, the primary mirror has approximately 0.4 waves rms of spherical aberration at 633 nm wavelength. The fact that the figure error is in the primary mirror, and not in the secondary, means that spherical aberration was introduced without the introduction of coma. This is critically important to the operation of the FGS since coma destroys the interference transfer function that is at the heart of the FGS function whereas spherical aberration does not. The spherical aberration does have some detrimental effect on the FGS, however (Ftaclas et al. 1993). This is because residual misalignments of the collimated beam on the Koester prisms cause the spherically aberrated wave front to be sheared by the Koester prism. Since the derivative of spherical aberration is coma, this shearing effect in the FGS mimics coma in the OTA. Fortunately, the amount of coma that has been introduced into the FGS by this mechanism is sufficiently small that it has not destroyed the observability of the transfer functions. But it has introduced an additional source of positional distortions that can and must be calibrated along with the OFAD. This source of distortion appears to be constant for a given secondary mirror position. It has an amplitude of approximately 10 mas and slowly varies across the FGS FOV. For the purposes of the OFAD calibration, the two sources of positional distortion, the optical design and the effect of a misaligned pupil combined with spherical aberration, are inseparable and so they are considered as a single distortion in our analysis.

Two additional sources of difficulty have been discovered since launch. First, for reasons that are not well understood at this time, the metrology of the FGS optical system has not fully stabilized. A post-launch period of change was expected since the metering structures are made of graphite epoxy which shrinks in a non-uniform way due to water desorption. While the amount of change that is observed has dramatically decreased since the first few months after launch, there remains a time varying part of the distortions that are observed by the FGS. We have had to

generalize our model and our calibration tests to account for these time dependent changes. The second source of difficulty that has been encountered is what appears to be short-term changes of the primary-to-secondary mirror despace that results in a focus shift over the *HST* orbit. The Wide Field and Planetary Camera, as well as the FGSs, have observed this phenomenon. It is hypothesized that the change in secondary mirror despace (also known as breathing) is caused by thermal variations during the 90 minute orbit, see Hasan and Burrows this volume. In the astrometry FGS it is predicted that changes in translation, roll and scale of the targets occur during an orbit as a result of the focus change. An effective observing strategy is to revisit three check stars several times over an orbit, in addition to the program stars. From the check star information an affine transformation can be computed that corrects for the effects of breathing. The negative aspect of this scenario is that it reduces the number of program stars that one can observe over the orbit.

Although there are three FGS interferometers on-board *HST*, the large amount of spacecraft time required to fully calibrate each unit led to the decision to designate one FGS as the astrometer and then to fully calibrate only that unit. An extensive set of tests was undertaken and analyzed. These tests resulted in the decision to choose FGS 3 as the astrometer (Benedict et al. 1992). The remainder of this paper deals with the calibration of FGS 3 exclusively.

II. The Determination of OFAD

ii.i. Overlapping plate method

Jefferys (1979) developed an overlapping plate method to determine the OFAD. The telescope would be pointed toward a rich field of stars, such as an open cluster, extending over approximately 30 arc minutes containing many stars with magnitudes ranging from 10 to 14. Measuring a set of stars which appear in the FGS field of view (colloquially known as a pickle because of its shape), we get an observational plate. Then we offset the telescope slightly, and do the measurement again to get another plate. These two plates contain several common stars, but the common stars will appear in different positions of pickle. If there were no distortion effects, the relative star positions from the two plates would be the same. In other words, any positional differences must be caused by distortion due to the measurements being made in different regions of the pickle. By observing many stars on many plates, we can find a model that best fits the data.

The criteria for choosing the total number of plates and the sizes of offsets are:

- the offsets should be large while including as many common stars as possible,
- the calibration should use as few plates as possible, while keeping the precision of the reduction at the desired level, since the observations are quite time-consuming.

After many simulations, we chose a set of 19 pointings as the baseline, which contains a central pointing, six small-offset pointings that are arranged in a hexagon that is 120 arcsec from apex to apex across the center, six larger-offset pointings

whose centers lie on the central radius of the pickle, and six rotated plates that are centered on the central pointing and on each of the middle pair of larger-offset pointings. The rotated plates were rotated as much as the roll constraints on the telescope would permit. For the time that the calibration was run (10 January 1993 UT), the maximum permissible rolls were +30° and –25°. Figure 1 shows the FGS fields of view for the 19 pointings projected onto the calibration star field in M35. The one pickle that is concave up represents the pointing we use during the fall (when the telescope has rolled through 180° due to solar array pointing constraint) to monitor the OFAD.

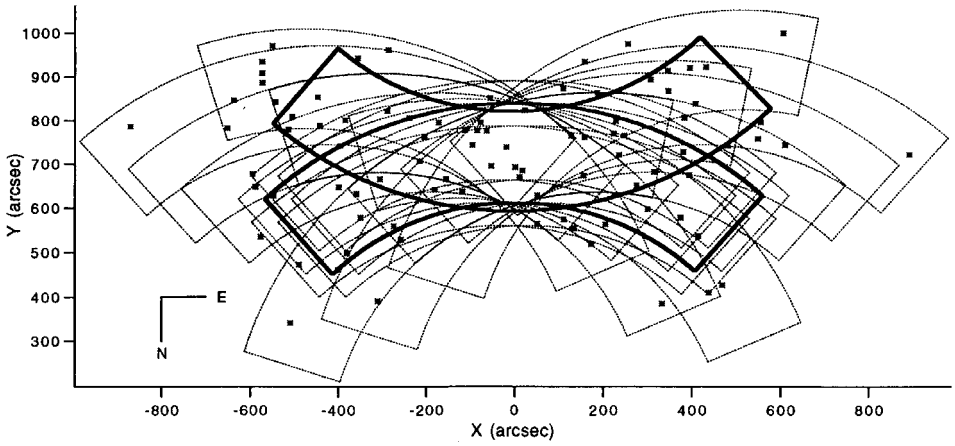

Figure 1: The geometry of the *HST* OFAD calibration. The positions of the stars used in the calibration indicated. The FGS field of view outlines are shown for the 19 successful orbits of the 10 January 1993 UT calibration run (concave down) as well as for the spring (concave down) and fall (concave up) LTSTAB tests.

ii.ii. The OFAD model

The statistical model for the OFAD can be expressed as:

$$Q_p^{\dagger}\hat{\xi}\, Q_p = \hat{x} + \Delta\hat{x} + \hat{\varepsilon} \tag{1}$$

where $\hat{x}$ is the observed position vector; $\hat{\xi}$ is the unknown parameter of star position vector; Q_p is an unknown quaternion for transforming the different plates to the reference plate (Jefferys, 1987); $\Delta\hat{x}$ includes systematic corrections of the pick-off, aspheric collimating, and upper and lower fold flat mirror figure errors, the velocity aberration, the telescope guiding errors, the star selector encoder (SSE) parameters, and the OFAD; $\hat{\varepsilon}$ is the random error (assumed Gaussian). Of the systematic corrections, those due to the pick-off, aspheric collimating, and upper and lower fold flat mirror figure errors, and the velocity aberration are known (in the case of the mirror figure errors, from pre-launch calibrations) and can be corrected as a part of the normal "pipelining" of the data. The remaining corrections due to the unknown (and possibly time dependent) SSE parameters, and the OFAD must be estimated

from on-orbit data. Finally, two sets of "nuisance" parameters must be estimated as well. These account for the pointing and guiding of the telescope during the calibration observations (and, for that matter, during science observations). All of these facets of our OFAD model are detailed below.

ii.iii. The catalogue position

When measuring the position of a star using the FGS, we must first transform its equatorial coordinates *a*, *d* from an existing relatively low-accuracy (~20 mas) star catalogue to the pickle coordinate frame $\hat{\xi}$. Since FGS astrometry involves relative measurements with respect to the V1 axis, we also need to choose a space orientation α_o, δ_o of the V1 axis and a roll angle θ_o around the V1 axis so that the desired star can be found in the pickle. There are several ways to do the coordinate transformation. Here we use the quaternion method developed by Jefferys (1987), in order to maintain consistency with the other parts of the data reduction. We first rotate coordinates from equatorial to the V1 axis frame $\hat{\xi}_s$:

$$\begin{bmatrix} 0 \\ \xi_s \\ \eta_s \\ \zeta_s \end{bmatrix} = Q_{es}^{\dagger} \begin{bmatrix} 0 \\ \cos\alpha\cos\delta \\ \sin\alpha\cos\delta \\ \sin\delta \end{bmatrix} Q_{es} \tag{2}$$

where the quaternion Q_{es} can be expressed as three consecutive rotations

$$Q_{es} = Q_{\alpha} \cdot Q_{\delta} \cdot Q_{\theta} \tag{3}$$

and where $Q_{es}^{\dagger}$ is the conjugate of Q_{es}, and

$$Q_{\alpha} = \begin{bmatrix} \cos\frac{\alpha_0}{2} \\ 0 \\ 0 \\ \sin\frac{\alpha_0}{2} \end{bmatrix}, \; Q_{\delta} = \begin{bmatrix} \cos\frac{-\delta_0}{2} \\ 0 \\ \sin\frac{-\delta_0}{2} \\ 0 \end{bmatrix}, \; Q_{\theta} = \begin{bmatrix} \cos\frac{\theta_0}{2} \\ \sin\frac{\theta_0}{2} \\ 0 \\ 0 \end{bmatrix}. \tag{4}$$

The next step is to transform the coordinates from the V1 axis to the i*th* FGS frame $\hat{\xi}$ that we are using:

$$\hat{\xi} = Q_i^{\dagger}\hat{\xi}_s Q_i \tag{5}$$

where the nominal values of the quaternion Q_i, i =1,2,3 for the three FGSs are:

$$Q_1 = \begin{bmatrix} \frac{\sqrt{2}}{2} \\ 0 \\ \frac{\sqrt{2}}{2} \\ 0 \end{bmatrix}, Q_2 = \begin{bmatrix} \frac{1}{2} \\ -\frac{1}{2} \\ \frac{1}{2} \\ -\frac{1}{2} \end{bmatrix}, Q_3 = \begin{bmatrix} 0 \\ \frac{\sqrt{2}}{2} \\ 0 \\ \frac{\sqrt{2}}{2} \end{bmatrix}. \tag{6}$$

The first component of the quaternion is the “scalar” or “real” part and the other three components comprise the “vector” or “imaginary” part. That is,

$$\begin{bmatrix} a \\ b \\ c \\ d \end{bmatrix} = a + b\hat{i} + c\hat{j} + d\hat{k}$$

with

$$\hat{i}\hat{j} = \hat{k} = -\hat{j}\hat{i}$$

$$\hat{j}\hat{k} = \hat{i} = -\hat{k}\hat{j}$$

$$\hat{k}\hat{i} = \hat{j} = -\hat{i}\hat{k}$$

As it will bear on our results concerning the relative positions of the stars that will be discussed in Section 4, it should be stressed here that the values of α_o, δ_o and θ_o cannot be estimated from the FGS data to a level of accuracy that is any better than the ground-based catalog that is used. Positional astrometry with the *HST*/FGS system is strictly relative, not absolute.

ii.iv. The correction for velocity aberration

Due to the space motion of *HST*, the measured positions will suffer a substantial amount of velocity aberration (about several arc seconds). Murray (1983) gives the relativistic vectorial expression for the aberration $\hat{a}(\hat{x})$:

$$\vec{x}_{true} = \vec{a}(\vec{x}) = \frac{\vec{\vec{L}}(\vec{x} + \vec{\beta})}{1 + \beta \cdot x} \tag{7}$$

where $\vec{\vec{L}}$ is the Lorentz tensor:

$$\vec{\vec{L}} = \frac{\vec{\vec{I}}}{\gamma} + \left(1 - \frac{1}{\gamma}\right)\frac{\hat{v}\hat{v}^T}{v^2} \tag{8}$$

with

$$\gamma = \frac{1}{\sqrt{1-\beta^2}}; \quad \vec{\beta} = \frac{\vec{v}}{c},$$

where c is the speed of light, and $\vec{v}$ is the space velocity of *HST* in the pickle frame, and v and β are the magnitudes of $\vec{v}$ and $\vec{\beta}$, respectively.

For relative measurements, the main effects of the aberration will cancel, and only the differential aberration is significant at the order of ±20 mas. Here the differential aberration refers to the aberration difference between some reference axis (the direction for which the absolute velocity aberration has been corrected) and the star which we are measuring:

$$\vec{x}_{true} = Q_t^{\dagger}\vec{a}(\vec{x})\,Q_t, \tag{9}$$

where $\vec{x}_{true}$ are the unaberrated coordinates, $\vec{x}$ are the aberrated ones, $\vec{a}(\vec{x})$ is the absolute aberration, and Q_t is the quaternion which rotates the coordinates of the aberrated reference axis to the unaberrated reference axis. Thus the corrections become,

$$\Delta\vec{x}_{aber}(\vec{x};a,e,i,\Omega,\omega,M_0) = \vec{x}_{true} - \vec{x}. \tag{10}$$

To determine the Q_t, we take the *HST* axis that was corrected for absolute velocity aberration as our reference axis, $\vec{x}_{ref}$, which by definition, suffers no differential aberration. Thus,

$$\vec{x}_{ref} = Q_t^{\dagger}\vec{a}(\vec{x}_{ref})\,Q_t. \tag{11}$$

ii.v. Pick-off and aspheric mirror figure error corrections

As with any optical surface, the as-built mirrors in the FGS are not perfect. Misfigured surfaces which are not near the system pupil produce slope (pointing) errors across the full aperture (see Figure 1 in Bradley et al. 1991 for the location of

the pupil). The FGS pick-off and aspheric mirrors are the main contributors to this type of distortion with an amplitude range of 2 to 5 mas. To a lesser extent the Star Selector A fold mirrors add to this effect.

Prior to FGS assembly, each mirror was tested interferometrically. The wavefront tilts, figure error, for individual subapertures were converted to object space distortions. By *HST*/FGS convention, object space refers to a celestial coordinate system that is rotated, but not projected, to be fixed to any of the three FGSs. The distortions were fit to the OFAD polynomial (see Section ii.x for the form of the polynomial). Much of the figure error was characterized by the polynomial. However, there existed locations in FGS FOV that contained high spatial frequencies in figure error. Hence, the residual errors in the polynomial fit were larger at these positions. In order to avoid this effect, the observed FGS data are corrected for the measured errors in the pick-off and aspheric collimating mirrors as part of the normal pipelining of the data.

ii.vi. Encoder errors

The 21 bit optical encoders in the Star Selector Assemblies cause small oscillatory errors in the reported positions due to the inevitable manufacturing imperfections in the encoder masks. These errors are repeatable and were characterized prior to launch. The 14 most significant bits contribute low frequency errors that are readily absorbed by the OFAD calibration. The errors that are associated with the 7 least significant bits have higher frequencies and cannot be accommodated by the OFAD. Consequently, a pre-launch calibration was used to generate a look-up table that is used to remove the least significant bit errors during the processing of the data.

ii.vii. Quaternions as plate constants

Using quaternions as plate constants, we can precisely transform a star vector from a standard plate $\hat{\xi}$ to the measured plate $\hat{x}$ without introducing any approximations (Jefferys, 1987):

$$\hat{x} = Q_p^{\dagger}\hat{\xi}Q_p, \tag{12}$$

where the quaternion Q_p satisfies $Q_p^{\dagger}Q_p = 1$.

ii.viii. Spacecraft jitter and drift correction

The normal function of the two guiding FGSs is to hold the spacecraft pointing fixed such that the guide star in the dominant FGS does not move and to hold the roll of the spacecraft fixed such that the guide star in the sub-dominant FGS is free to move only along the line that passes through it and the dominant guide star. The details of the operation of the Pointing Control System are given in Bradley et al. (1991). For a variety of reasons, the guiding of the telescope during the course of the observations (≈30 minutes) is not perfect at the level of a millisecond of arc. To remove any

residual guiding errors we have implemented a de-jitter algorithm that measures and corrects the instantaneous deviation of the spacecraft pointing from an arbitrary but fixed reference frame. The fixed reference frame is set by the guide star centroids measured during the fine lock interval of the first observation in the plate. For all the other observations in the orbit, any change in the guide star centroids is interpreted as due to vehicle jitter which is then removed from the astrometry star centroid. Specifically, the de-jitter algorithm assumes that any motion of the dominant guide star is due to pure spacecraft translation and that any motion of the sub-dominant star along a direction perpendicular to the line between the guide stars (after spacecraft translation is removed) is vehicle roll.

We have also observed drift of stars in the astrometry FGS relative to the guiding FGSs. This relative motion is thought to be due to a combination of the breathing effect alluded to earlier and thermal effects associated with the FGSs. The solution to this problem is to include in the observation set a series of check stars that are revisited throughout the observation set. For the OFAD calibration, we included three stars in each plate that we observed, in sequence, at the beginning and end of the orbit as well as individually during the central part of the orbit. For example during the observation at the central pointing, the identification numbers, in our numbering system, of the check stars were 862, 853, and 894. Star 862 was observed 1st, 15th, and 30th; star 853 was observed 2nd, 9th, 20th, and 29th, and star 894 was observed 3rd and 28th during the total plate of 30 observations. We used a solid body linear drift model (i.e. FGS 3 was assumed to move as a solid body with constant velocity and no rotation relative to the two guiding FGS units) of the form

$$\Delta\dot{x}_{drift}\left(\dot{x}_i;\dot{\dot{x}}_j\right) = \dot{\dot{x}}_j\,(t_i - t_{1j})\,, \tag{13}$$

where j is the plate number, i is the star number within the jth plate, t_i is the time of the observation, and t_{1j} is the time of the first observation in the jth plate. Note that if there is only one observation of a given star on a particular plate (i.e. the star is not a check star) then the position of that star changes but it does not contribute any information to the estimation of the drift.

ii.ix. The correction to SSE

The correction, $\Delta\dot{x}$, due to incorrect initial values of the SSE parameters is:

$$\Delta\dot{x}_{SSE}\,(\dot{x};\rho_A,\rho_B,k_A,k_B,M) = \dot{x}_{true} - \dot{x}. \tag{14}$$

From Figure 2, we see that the raw data of FGS observation are the measurements of the rotation angles of the two star selectors θ_A, θ_B. The Cartesian coordinates, in object space, $\dot{x}$, are derived by using the initial parameter values which may not be well determined. To include any possible corrections for the SSE, we should first convert the $\dot{x}$ back to θ_A, θ_B using the nominal values, then by letting the parameters vary freely, convert them back to get $\dot{x}_{true}$.

The polar coordinates, ρ and ϕ, of $\dot{x}$ are given by:

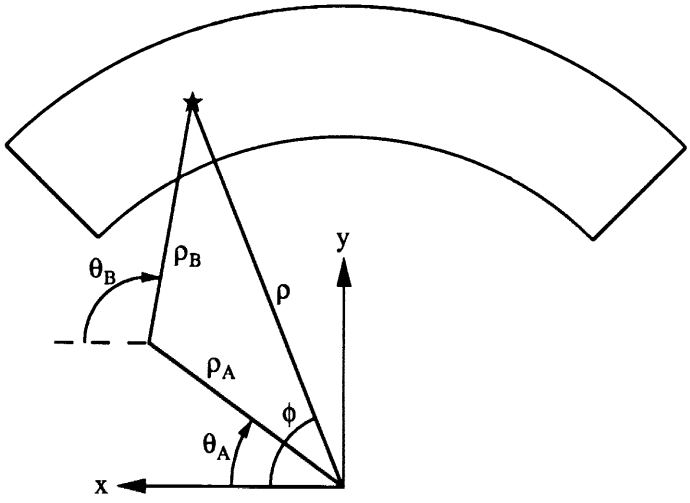

Figure 2: The coordinate system used in *HST* FGS observations.

$$\tan\frac{\rho}{M^o} = \sqrt{\frac{x^2+y^2}{z^2}}$$
$$\tan\phi = \frac{y}{x} \tag{15}$$

and have a spherical trigonometrical relation with θ_A, θ_B (Fresneau, 1985):

$$\cos(180^\circ - q) = \frac{\cos\rho - \cos\rho_A^o\cos\rho_B^o}{\sin\rho_A^o\sin\rho_B^o}$$
$$\cos p = \frac{\cos\rho_B^o\sin\rho_A^o - \sin\rho_B^o\cos\rho_A^o\cos(180^\circ - q)}{\sin\rho} \tag{16}$$

with $\theta_A = \phi - k_A^o - p$ and $\theta_B = q - k_B^o + (\theta_A + k_A^o)$, where the nominal values of the SSE parameters are: $M^o = 57.3$; $\rho_A^o = \rho_B^o = 6.7758^\circ$; $k_A^o = k_B^o = 0$.

Now we transform the raw θ_A, θ_B back to $\grave{x}_{true}$ using the free parameters ρ_A, ρ_B, k_A, k_B and M:

$$\begin{aligned}
\cos\rho' &= \cos\rho_A\cos\rho_B + \sin\rho_A\sin\rho_B\cos(180^\circ - q) \\
\sin\rho'\sin p &= \sin\rho_B\sin(180^\circ - q) \\
\sin\rho'\cos p &= \cos\rho_B\sin\rho_A - \sin\rho_B\cos\rho_A\cos(180^\circ - q)
\end{aligned} \tag{17}$$

with $q = (\theta_B + k_B) - (\theta_A + k_A)$ and $p = \phi' - \theta_A - k_A$. Converting ρ', ϕ' to rectangular coordinates, we obtain $\hat{x}_{true}$:

$$\begin{aligned}
x_{true} &= \sin\frac{\rho'}{M}\cos\phi' \\
y_{true} &= \sin\frac{\rho'}{M}\sin\phi'
\end{aligned} \tag{18}$$

ii.x. The correction for OFAD

We may reasonably represent the OFAD correction by two low-order polynomials in the pickle frame:

$$\begin{aligned}
\Delta x_{dist}(x,y;a_{ij}) &= x_{true} - x = \sum_{i=0}^{5}\sum_{j=0}^{5} a_{ij}x^i y^j \\
\Delta y_{dist}(x,y;b_{ij}) &= y_{true} - y = \sum_{i=0}^{5}\sum_{j=0}^{5} b_{ij}x^i y^j
\end{aligned} \tag{19}$$

where a_{ij}, b_{ij} are a set of constant coefficients to be determined. The actual functional form of the polynomial used is somewhat different. The largest distortion, contributed by the classical design of the aligned powered elements in the OTA/FGS system, has a well-known signature. It is a simple 5th order polynomial that is a function of the sine of the optical field angle, ρ (the radial component of Eq. 18):

$$\Delta_{dist} = \sin\rho_{true} - \sin\rho = a(\sin\rho)^3 + b(\sin\rho)^5. \tag{20}$$

In Cartesian coordinates, this design distortion is cast into the form:

$$\Delta x_{dist}(x,y;a,b) = x_{true} - x = ax(x^2+y^2) + bx(x^2+y^2)^2$$

$$\Delta y_{dist}(x,y;c,d) = y_{true} - y = cy(x^2+y^2) + dy(x^2+y^2)^2 \tag{21}$$

Misaligned optical elements break the symmetry, add a DC bias, add distortion, and require additional terms in the polynomial. The equations that are actually used for our modeling of the OFAD are:

$$\begin{aligned}\Delta x_{dist}(x,y;a_{ij}) = x_{true} - x = {} & a_{00} + a_{10}x + a_{01}y + a_{20}x^2 + a_{11}xy + a_{30}x(x^2+y^2) \\ & + a_{21}x(x^2-y^2) + a_{12}y(y^2-x^2) + a_{03}y(y^2+x^2) \\ & + a_{50}x(x^2+y^2)^2 + a_{41}y(y^2+x^2)^2 + a_{32}x(x^4-y^4) \\ & + a_{23}y(y^4-x^4) + a_{14}x(x^2-y^2)^2 + a_{05}y(y^2-x^2)^2\end{aligned}$$

$$\begin{aligned}\Delta y_{dist}(x,y;b_{ij}) = y_{true} - y = {} & b_{00} + b_{10}x + b_{01}y + b_{20}x^2 + b_{11}xy + b_{30}x(x^2+y^2) \\ & + b_{21}x(x^2-y^2) + b_{12}y(y^2-x^2) + b_{03}y(y^2+x^2) \\ & + b_{50}x(x^2+y^2)^2 + b_{41}y(y^2+x^2)^2 + b_{32}x(x^4-y^4) \\ & + b_{23}y(y^4-x^4) + b_{14}x(x^2-y^2)^2 + b_{05}y(y^2-x^2)^2\end{aligned} \tag{22}$$

where the coefficients a_{ij}, b_{ij} are the constants that are estimated. From Eq.(22), we can see that the variables x and y are mixed together and both have their own observation errors. This is the errors-in-variables problem which has been discussed by Jefferys (1990).

ii.xi. The constraints

There is insufficient information in the *HST* observations alone to permit the adjustment of the full set of SSE parameters, M, ρ_A, ρ_B, and k_B. Without additional information, the least-squares problem would be singular and the iteration procedure would diverge. So, we introduce an external source of scale information, such as a ground-based catalog, and constrain the estimated scale to approximate the implicit scale of the ground-based catalog. Moreover, our *a priori* knowledge of the plate scale is quite good (approximately one part in 1000) so that we can start the least-squares estimation quite close to the best-fit solution.

In addition to the above constraint, we still have to consider other constraints to arrive at a unique result, due to the fact that we do not want the linear terms in the distortion correction to introduce any additional translation, rotation or scale change. To make this clear, we express our model explicitly in terms of plate constants:

$$\begin{aligned} a\xi + b\eta + c &= x - \Delta x_{dist}(x,y;a_{ij}) - \Delta x(M,\rho_A,\rho_B,k_B) \\ -b\xi + a\eta + d &= y - \Delta y_{dist}(x,y;b_{ij}) - \Delta y(M,\rho_A,\rho_B,k_B) \end{aligned} \tag{23}$$

The constant and linear terms in the distortion are mixed with a, b, c, d of the plate constants. So we apply the following gauge constraints:

$$a_{00} = b_{00} = 0;\ a_{10} = b_{01};\ a_{01} = b_{10} = 0, \tag{24}$$

to separate the distortion coefficients from the plate constants. The ability to include arbitrary equality constraints is a feature of the GaussFit program we used to implement our algorithm (Jefferys et al. 1988).

Finally, since there is a linear relationship between θ_A, θ_B, k_A, and k_B, only one clocking error, k_A, is estimated. The value of k_B is constrained to be zero.

ii.xii. The condition equations

Let l be the number of stars observed, n be the number of observations in each plate, and m be the number of the plates. The total number of unknowns involved in the model is the sum of: four quaternion components for each plate ($4m$), two drift parameters for each plate ($2m$), a variable number ($\approx$30) of distortion coefficients a_{ij}, b_{ij}, the star-selector-deviation parameters ρ_A, ρ_B, k_A, and two components of star position for each star (2l).

The OFAD is solvable if the total number of the equations is larger than the number of unknowns. Let us roughly estimate these two numbers: suppose we have m=20 plates, each of which contains n=30 observations. The total number of equations is $2mn$=1200. Because of the overlapping plates, every star is observed on at least two plates. In fact, if a star were observed on only one plate it would not contribute any information to the OFAD determination. As designed, the calibration in M35 required the estimation of the positions of l=93 stars. So the number of expected unknowns was approximately $4m+2m+30+3+2l$ = 339 and the least squares problem was well determined.

III. The *HST* Observations

The OFAD calibration actually began in December 1990 with the first of a series of mini-OFADs that were performed to improve the knowledge of the FGS-to-FGS alignments as well as the observed distortions. These calibrations were made to support the general operation of the spacecraft and differed from the full-OFAD calibration in that the positions of the stars were assumed to be known at the 10's of

milliseconds of arc level and were held fixed in the estimation. This simplification meant that the mini-OFAD calibrations required far less telescope time than the full-OFAD (typically a few orbits as opposed to 20). The mini-OFAD calibrations not only succeeded in providing the information needed to accurately point to targets with the small apertures in the other science instruments, but it also revealed time dependent changes in the OFAD. The observations were not of sufficient quality, nor were they made often enough (6 to 12 months was typical of the time between mini-OFADs) to fully resolve the nature of these changes but it appeared that the changes could be modeled, to the accuracy of the data, by a time dependent change in ρ_A.

This discovery prompted us to begin a series of long-term stability tests (LTSTAB for short) to monitor any changes in the OFAD. The monitoring effort consists of periodic visits (ideally once per month) to the M35 field used for the OFAD. In fact, M35 was chosen for the OFAD calibration because of the need to run the LTSTAB tests. Since M35 is in the ecliptic, the telescope does not gradually roll about this field throughout the year as it does for a target off the ecliptic. Instead, the telescope flips 180° when M35 gets closest to the anti-solar point (to be precise, the telescope rolls 180° between December 20 and December 28 with the bulk of the roll occurring on December 24). This means that we can observe the calibration field at two fixed orientations; one in the fall and one in the spring. This maximizes our sensitivity to real changes in the OFAD and minimizes our sensitivity to uncertainties in the OFAD that might appear as changes if the telescope gradually rolled through the calibration field. Each spring the LTSTAB test consists of a single orbit of observations that repeat the central pointing of the OFAD. The fall LTSTAB tests also consist of a single orbit of observations but are rolled approximately 180° about the central pointing of the OFAD calibration. These two pointings are highlighted by the heavy lines in Figure 1. Two executions of the LTSTAB test were made before the OFAD calibration; on December 2 and 14, and three were run after the OFAD calibration; on April 5, 18, and 19. We expect to continue the LTSTAB tests, at a rate of approximately once per month, whenever M35 is observable.

The analysis presented in this report concerns only the 20 orbit OFAD calibration executed on 10 January 1993. The analysis of the OFAD plus LTSTAB data (what has come to be called a grand-OFAD) is still in progress. The preliminary conclusion of that analysis is that the changes that are occurring in the OFAD are of sufficiently low frequency that they can be modeled by changes in the SSE parameters. Consequently, it is meaningful to establish a baseline OFAD calibration from the 10 January 1993 spacecraft run. That is the purpose of this report. Subsequent reports by us will provide the means to model the time changing OFAD, for example by osculating SSE parameters or by a time dependent model and coefficients for the SSE parameters. We do not expect to have to change the coefficients of the 5th order OFAD polynomial.

The OFAD calibration itself occurred over 33 hours beginning on 10 January 1993. The calibration test consisted of 20 orbits. The central pointing was repeated on orbits 2 and 20 to permit us to monitor the stability of the OFAD over this period. The data from orbits 16 (one of the middle-sized large offsets at the nominal roll) and 20 were severely corrupted by problems with the spacecraft guiding. Fortunately, the de-jitter algorithm described in Sec. ii.viii completely recovered the data from orbit 16. It may be possible to recover the data from orbit 20 but they have not been

included in the analysis presented in this paper. On the whole, the telescope guiding was extremely good and a total of 525 observations (out of a possible 540) of 91 stars (out of a possible 93) were usable.

IV. Results from our Analysis of the OFAD Data

We have subjected the data from the 19 uncorrupted orbits from the OFAD calibration run in January 1993 to the analysis described in Section 2. We estimated the relative positions of the stars, the SSE parameters M, ρ_A, ρ_B and k_A, and the OFAD coefficients a_{ij} and b_{ij} simultaneously. Of course, in addition, the nuisance parameters of the plate quaternions and the drift parameters were estimated for each orbit.

TABLE 1. Estimated OFAD parameters for Hubble Space Telescope Fine Guidance Sensor Number 3. The meaning of the parameters is explained in the text. The columns labeled with σ's are the estimated variances of the parameters from the least squares solution. Parameters with zero variance were held fixed. The units for the coefficients a_{ij} and b_{ij} are arcseconds, the units for ρ_A, ρ_B, k_A, and k_B are degrees. The magnification, M, is dimensionless. All values are given with more figures than are significant to avoid truncation errors in the evaluation of the series.

i	j	a_{ij}	b_{ij}	σ_a	σ_b
0	0	0	0	0	0
1	0	-3.45958E-06	0	0	0
0	1	0	-7.59297E-06	0	0
2	0	-0.12955214	0.36034647	0.013	0.073
1	1	0.533394636	-0.050252249	0.27	0.042
0	2	-0.129174425	0.932529323	0.029	0.19
3	0	-486.7902615	21.6245827	33	6.9
2	1	44.18062474	-7.483542931	32	3.3
1	2	-12.75565183	-12.48193571	1.3	14
0	3	21.75969958	-632.8467698	6.6	32
5	0	1757942.554	0	3.4E+05	0
4	1	0	4380733.583	0	3.9E+05
3	2	-113432.3267	0	5.6E+05	0
2	3	0	600275.9563	0	3.3E+05
1	4	505077.8006	0	2.5E+05	0
0	5	0	-387380.1344	0	1.6E+05

		σ
ρ_A	6.90375608	0.010
ρ_B	6.90184945	0.010
k_A	-0.6767212	0.0094
k_B	0	0
M	57.3573493	0.086

The estimated values of the SSE parameters and the OFAD coefficients a_{ij} and b_{ij} are given in Table 1 along with the formal variances, from the least squares estimation, for each. The nonlinear part of the OFAD distortions are shown in Figure 3. Since the OFAD calibration is insensitive to absolute scale, the variances of all scale-like quantities, such as M and ρ_A, are inherently large. The rms of the residuals from the 548 individual observations from the OFAD orbits are 2.3 mas along both the x and y axes. This corresponds to an RSS error in a single observation of 3.2 mas over the entire field of view of the FGS. This is very close to the pre-launch expectation of 2.7 mas.

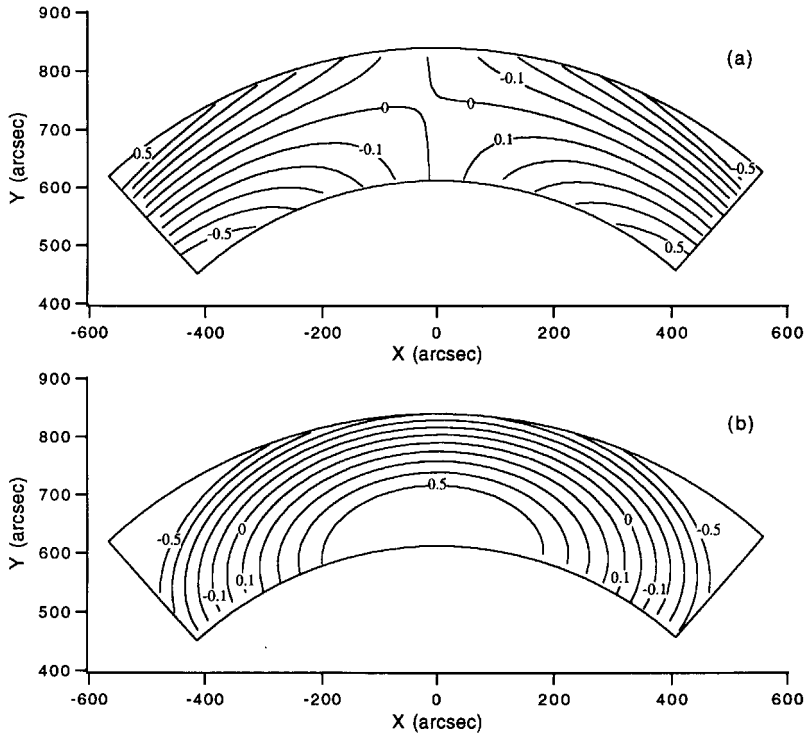

Figure 3: The nonlinear optical field angle distortions due to the *HST* optical telescope assembly as it is convolved with FGS number 3. The contours are labeled with the amount of distortion, in arcseconds, in the x (a) and y (b) coordinates.

It has already been stated that, since there is no field of stars whose relative positions are known to the level of accuracy required for the *HST* OFAD calibration, we have had to estimate the star positions simultaneously. This means that we have the first catalog of relative star positions that are accurate to about 2 mas. Of course, the absolute positions of these stars are only known to the accuracy of the ground-based catalog to which we have referenced the relative positions. For this we used an updated version of McNamara and Sekiguchi's (1986) catalog. Our catalog of 91 stars in M35 is summarized in Table 2. We have tabulated values for the absolute right ascension, declination, and the V magnitude purely for reference and identification purposes. The new results being presented here are the relative coordinates x and h which are given with their estimated variances which were derived from the bootstrap analysis that is described in the next section.

V. Bootstrap Analysis of Bias and Variance

v.i. The definition of bias

The OFAD model Eq. (22) is nonlinear, and nonlinear least squares solutions may be affected by bias. Bias is defined as the difference between the *true T* and the expectation of the *estimated* values *R* of parameters:

$$Bias = E(R) - T \tag{25}$$

The causes of bias may be due to:

- use of the normal assumption when noise is not normal,
- nonlinearities in the model,
- neglect of important systematic effects.

In many practical cases, it is impossible to make the same observations many times to get the mean of solution $E(R)$. Furthermore, we don't know the true values (that's what we want to estimate). Therefore the usual least squares method cannot give a bias estimation.

v.ii. The bootstrap method

Efron's bootstrap method can be used to estimate bias due to causes (1) and (2) (Efron 1982, Wang 1990). The basic idea is as follows:

1. Estimate OFAD parameters $\hat{\theta}$ from the actual data by ordinary least squares fitting. Denote this reference solution as R.

2. Construct an observed-minus-calculated ($O - C$) residual bank from the R solution:

$$r = (O - C) = y - \hat{y} = -Bias + e, \text{ with } E(e) = 0 \tag{26}$$

3. Resample a new set of "observational" data by randomly drawing r from the residual bank with replacement:

$$Y^* = \hat{y} + r = y + e', \text{ with } E(e') = 0 \tag{27}$$

so Y^* is expected to have a bias with respect to the R solution.

4. Estimate the parameter θ again using the same OFAD model:

$$\hat{\theta}^* = \hat{\theta} + Bias + e^*, \text{ with } E(e^*) = 0 \tag{28}$$

Denote the bootstrap solution $\hat{\theta}^*$ as B.

5. Repeating steps (3) and (4) with independent samples a large number of times N, we get the sample mean $E(B)$. The estimate of the bias becomes:

$$\hat{Bias} = E(B) - R \tag{29}$$

From the basic bootstrap assumption $\hat{Bias} \approx Bias$, we equate Eq. (25) to Eq. (29), and obtain the bias-corrected parameter:

$$\hat{T} = R - (E(B) - R) . \tag{30}$$

It follows that

$$E(\hat{T} - T)^2 \approx \sigma_R^2 < E(R - T)^2 \approx \sigma_R^2 + E(Bias)^2 \tag{31}$$

This formula is the basis for our bootstrap analysis.

vii.iii. Checking the assumptions

For practical applications, we use the sample mean and variance to approximate the expectation and variance:

$$E(B) \approx \bar{B} = \frac{1}{N}\sum_{k=1}^{N} B_k, \tag{32}$$

$$\sigma_B \approx \hat{\sigma}_B = \sqrt{\frac{1}{N-1}\sum_{k=1}^{N}(B_k - \bar{B})^2}, \tag{33}$$

$$\sigma_{\bar{B}} = \sqrt{\frac{1}{N(N-1)}\sum_{k=1}^{N}(B_k - \bar{B})^2}, \tag{34}$$

when $N \to \infty$, $\hat{\sigma}_{\bar{B}} \to 0$ and $\bar{B} = E(B)$, while $\hat{\sigma}_B \to$ constant.

We may naturally raise the question: how can we determine N to fulfill our precision of $\bar{B} \to E(B)$? From sampling theory, if a single sample gives the precision $\hat{\sigma}_1$, then K groups of total N samples give the precision:

$$\hat{\sigma}_N = \frac{\hat{\sigma}_1}{\sqrt{N}} = \frac{\hat{\sigma}_1}{\sqrt{kK}} = \frac{\hat{\sigma}_k}{\sqrt{K}} \tag{35}$$

So if we have sampled a group with k replications and get a precision of $\hat{\sigma}_k$, and we are asking a precision of, say, $\hat{\sigma} \le 0.1\bar{B}$, the K (and so for $N = kK$) value can be estimated by

$$\frac{\hat{\sigma}_k}{\sqrt{K}} = 0.1\bar{B},\ K = \left(\frac{\hat{\sigma}_k}{0.1\bar{B}}\right)^2. \tag{36}$$

Applying the above to our situation, we have only one OFAD trial R and we have made 120 bootstrap replications B.

v.iv. Variance as a function of position

The bootstrap method can also provide a method to estimate the variance $\hat{\sigma}_R$ of the parameter $\hat{\theta}$ over whole pickle.

1. To get the variance as a function of position, we generate 100 uniform grid points $\grave{x}$ within the pickle by using

$$x_i = \rho_{i'}\cos\theta_{j'};\ y_i = \rho_{i'}\sin\theta_{j'};\ i = 1,100,\ i' = 1,5;\ j' = 1,20. \quad (37)$$

2. Calculate residuals between the reference solution R and the kth bootstrap solution B_k (k=1,2,...,N) for the ith (i=1,100) grid point:

$$\grave{r}_{ik} = \Delta\grave{x}(\grave{x}_i;B_k) - \Delta\grave{x}(\grave{x}_i;R) \quad (38)$$

3. Summing over N bootstrap replications, we estimate the bias and the variance for the ith point:

$$\hat{Bias}_i = \frac{1}{N}\sum_{k=1}^{N} r_{ik} \quad (39)$$

$$\hat{\sigma}_{B_i} = \hat{Var}_i = \sqrt{\frac{1}{N}\sum_{k=1}^{N}(r_{ik} - \bar{r}_{ik})^2}. \quad (40)$$

4. Applying the bootstrap assumption: $\hat{\sigma}_{R_i} \approx \hat{\sigma}_{B_i}$, we obtain an estimate of the variance $\hat{\sigma}_R$ over all pickle points. The contour maps for the reduction variance from Eq. (40) over a uniform grid can tell us about which region is most suitable for astrometry. Figure 4 shows that the expected error introduced into a star position by the derived OFAD will be less than 2 mas over almost the entire FGS field of view.

v.v. Variance of estimated parameters

The formal variances that are calculated as part of the least squares estimation are too large due to large correlations between the parameters. This is a particular problem with the star positions in the OFAD analysis. Since the positions of all of the stars depend in the same SSE parameters and OFAD coefficients they are all highly correlated. Consequently, we have calculated the variances of the estimated star positions using the bootstrap method just described. These variances are given in Table 2. We have performed similar calculations for the SSE parameters and found

that the variances that are calculated by the standard least squares method and the bootstrap method agree quite well.

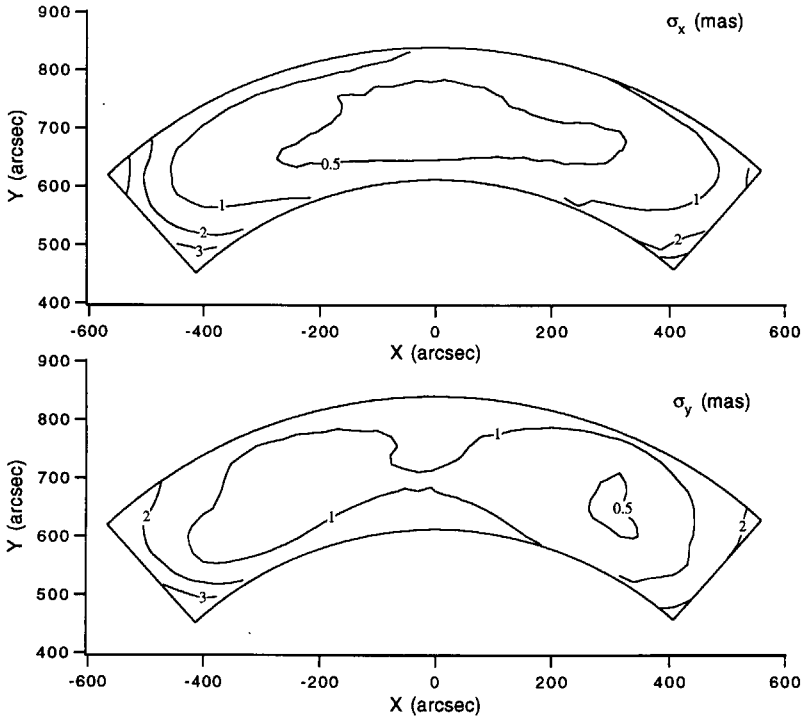

Figure 4: The expected error that will be introduced into a reduced FGS number 3 observation, due to the uncertainty in the OFAD polynomial, as calculated by a bootstrap analysis. Note that the root-sum-square contribution of the OFAD uncertainty is less than two milliarcseconds over almost the entire field of view.

VI. Remaining Work and Conclusions

As has already been stated, the data LTSTAB orbits were not included in the analysis described in this report. That analysis is on-going and an interim report is being released concurrently with this report.

Beyond the time dependence of the OFAD, the most significant unresolved issue concerning the OFAD is that of a possible lateral color effect. If there are significant lateral color effects in the FGS then they should be separately calibrated and the OFAD data re-analyzed to take these effects into account. In fact, a lateral color calibration was run on 23 December 1991. However, so much time elapsed between the execution of the lateral color and the OFAD calibrations that it has proven very difficult to connect the two calibrations. This analysis is still in progress.

The plate scale of the OTA/FGS system must be calibrated as well. This can be done in any of several different ways. Two methods that have been suggested are by use of stars that are part of the HIPPARCOS spacecraft catalog or by use of the motion of a minor planet. A calibration by the first method was begun in the spring of 1993 and

should yield a value for the plate scale that is accurate to a few milliseconds of arc over the FGS field of view.

Finally, the OFAD calibration that has been described here was made using the F583W filter. This filter is an essentially clear filter that has a pass band that is about 2340Å wide and is centered on 5830Å. FGS 3 has four other filters that can be used. They are a 2/3 pupil stop and red, yellow, and neutral density filters. Precise positional astrometry with any of these filters will require a cross filter calibration so that the OFAD measured with the clear filter can be used with the other filters.

The Astrometry Science Team is supported by NASA Grant No. NAG5-1603. The authors warmly acknowledge the interactions we have had, over many years, with Gary Welter, of Computer Sciences Corporation. Dr. Welter has done an immense amount of work on the operational calibration of the FGS and he has been an invaluable asset toward our scientific calibration. We are also grateful to J. Keith Kalinowski, of NASA/GSFC, for his many useful suggestions about the design and execution of the OFAD calibration observations.

References

Benedict, G.F. et al. 1992, PASP 194, 958

Bradley, A., Abramowicz-Reed, A., Story, D., Benedict, G. & Jefferys, W. 1991, PASP 103, 317

Burrows, C.J. et al. 1991, ApJ 369, L21

Cudworth, K.M. 1971, AJ 76, 475

Efron, B. 1982, The Jackknife, the Bootstrap and Other Resampling Plans, SIAM, Philadelphia

Fresneau, A. 1985, Hubble Space Telescope Fine Guidance Sensors Instrument Handbook, The Space Telescope Science Institute, Baltimore

Ftaclas, C. et al. 1993, Ap. Opt. 32, 1696

Jefferys, W.H. 1979, AJ 84, 1775

Jefferys, W.H. 1987, AJ 93, 755

Jefferys, W.H. 1990, Biometrika 77, 597

Jefferys, W.H., Fitzpatrick, M.J. & McArthur, B.E. 1988, Celest. Mech. 41, 39

Lasker, B.M., Jenkner, H. & Russell, J.L. 1988, in IAU Symp. No. 133, Mapping the Sky-Past Heritage and Future Directions, eds. S. Debarbat et al., Kluwer, Dordrecht, p. 229.

McNamara, B. and Sekiguchi, K. 1986, AJ 91, 557

Murray, C.A. 1983, Vectorial Astrometry, Adam Hilger, Bristol, p. 21

Wang, Q. 1990, Statistical Analysis of OFAD of *HST* using Bootstrap Method, M.A. Thesis, The University of Texas at Austin

TABLE 2. Estimated positions of the stars from 19 orbits of HST data taken for the OFAD calibration. The star numbers labeled MS# and CD# refer to the indices used by McNamara and Sekiguchi (1986) and Cudworth (1971), respectively. We have calculated absolute positions from the estimated relative positions ξ, η using $\alpha_o = 92.^{\circ}28890496$, $\delta_o = 24.^{\circ}58078484$, $\theta_o = 89.^{\circ}817036$. The V magnitudes were obtained from the *Hubble Space Telescope Guide Star Catalog* (Lasker, Jenkner, and Russell 1988) and are intended as an aid in identification only.

#	MS#	CD#	ξ	η	σ_ξ	σ_η	α (J2000)	δ	V
81			872.5462	791.9500	0.0027	0.0076	92.02207053	24.36133785	13.51
9			653.7647	786.2973	0.0015	0.0044	92.08878648	24.36281700	13.25
572			638.2968	850.2741	0.0023	0.0049	92.09346830	24.34503800	12.23
906			597.5594	680.1915	0.0019	0.0036	92.10598600	24.39226282	12.02
877			590.9608	652.0120	0.0014	0.0033	92.10801482	24.40008706	12.00
856			579.5590	538.8209	0.0030	0.0040	92.11155869	24.43152309	13.52
627			574.8319	912.4411	0.0018	0.0037	92.11278156	24.32773673	10.13
628			574.7750	937.5631	0.0031	0.0041	92.11278416	24.32075832	11.66
543			574.5118	889.8787	0.0024	0.0043	92.11289240	24.33400394	10.93
584			551.5653	974.9426	0.0032	0.0040	92.11983663	24.31036252	12.01
883			550.1506	630.4773	0.0020	0.0033	92.12047582	24.40604712	12.39
419			545.1814	845.7430	0.0017	0.0032	92.12186093	24.34624809	12.07
629			515.7988	782.6117	0.0019	0.0032	92.13085905	24.36376822	10.84
876			513.0989	344.4630	0.0033	0.0035	92.13195765	24.48547489	11.73
539			506.4927	811.7363	0.0014	0.0027	92.13367834	24.35567269	10.40
951			492.8937	476.1573	0.0030	0.0034	92.13804033	24.44888148	9.74
712			448.3656	856.8739	0.0016	0.0022	92.15137180	24.34310001	12.59
714	99	255	443.2047	791.5481	0.0013	0.0020	92.15298938	24.36124300	11.99
886			404.1424	463.1985	0.0023	0.0024	92.16513092	24.45242699	13.17
967	114	272	401.6386	649.8831	0.0010	0.0015	92.16576365	24.40056851	9.91
985	116	274	397.4187	744.4405	0.0010	0.0015	92.16698405	24.37429978	12.27
756	120	277	385.8561	803.5714	0.0012	0.0017	92.17046797	24.35786702	12.04
972			383.9666	500.8326	0.0021	0.0020	92.17126059	24.44196010	13.64
897	129	284	360.9692	634.3715	0.0018	0.0019	92.17818005	24.40485083	12.98
614	130	287	356.2041	946.7008	0.0019	0.0019	92.17940445	24.31808912	11.89
894	134	288	351.5530	580.3633	0.0010	0.0013	92.18109210	24.41984685	10.22
934			313.5950	393.3687	0.0026	0.0022	92.19281446	24.47176391	11.48
948	155	312	307.1579	667.5615	0.0008	0.0009	92.19456881	24.39559475	11.68
514	163	317	289.9747	824.8970	0.0011	0.0011	92.19968745	24.35187823	11.64
520	165	318	286.9921	964.1637	0.0028	0.0028	92.20048826	24.31319070	11.36
978	171	323	277.0894	560.8813	0.0012	0.0012	92.20382394	24.42520694	12.54
919	179	331	261.1165	530.6333	0.0014	0.0015	92.20872108	24.43359766	9.33
817	188	337	240.4090	807.7547	0.0012	0.0011	92.21481413	24.35660420	10.91
975	196	345	217.2856	708.7570	0.0006	0.0007	92.22194667	24.38408643	12.85
607	203	350	206.4610	763.7732	0.0008	0.0007	92.22520208	24.36879594	10.87
947	213	363	183.6265	643.8614	0.0007	0.0008	92.23226719	24.40208734	11.05
509	218	371	173.7209	797.3821	0.0008	0.0008	92.23515723	24.35943494	8.08
964	220	374	157.9684	667.1567	0.0008	0.0008	92.24007335	24.39559638	10.47
845	240	389	121.2729	637.6745	0.0008	0.0009	92.25129212	24.40375654	11.66
688	243	393	115.0819	778.7659	0.0017	0.0018	92.25305425	24.36455941	9.88
732	247	398	97.1370	744.8082	0.0006	0.0007	92.25855705	24.37397739	10.63
729	250		86.7727	778.7618	0.0014	0.0013	92.26168670	24.36453721	11.69
737	251		78.6382	797.0761	0.0008	0.0009	92.26415032	24.35944312	12.23
478	254	405	65.6711	777.2251	0.0009	0.0011	92.26812270	24.36494639	13.09
554			56.6148	852.6930	0.0011	0.0011	92.27081379	24.34397534	11.50
912			55.0977	696.4795	0.0006	0.0010	92.27142243	24.38736678	12.35
853	277	427	20.6260	739.8682	0.0005	0.0009	92.28189433	24.37528463	10.25
875	288	434	0.5456	694.3468	0.0016	0.0019	92.28806231	24.38791184	12.35
932	294	439	-8.7250	670.8286	0.0006	0.0010	92.29091275	24.39443644	11.15
868	297	443	-14.9165	686.2715	0.0010	0.0014	92.29278604	24.39014121	10.95
710	298	445	-21.3444	824.6293	0.0009	0.0012	92.29461003	24.35170265	13.26
946	315	458	-47.8180	564.5539	0.0030	0.0026	92.30294314	24.42392185	12.09
918	316	459	-48.5950	629.0164	0.0007	0.0012	92.30311537	24.40601490	10.00
674	338	486	-107.8883	873.5249	0.0014	0.0014	92.32094646	24.33804046	9.36
885	341	488	-107.6786	574.0248	0.0021	0.0024	92.32119534	24.42123515	13.27
496	350	500	-125.5687	764.3660	0.0008	0.0011	92.32645196	24.36834549	9.79
980	361	510	-153.3241	674.2172	0.0006	0.0010	92.33501269	24.39335986	11.05
631	364	513	-156.2286	760.9498	0.0006	0.0009	92.33580515	24.36926465	10.69
687	363	514	-157.0757	934.4278	0.0021	0.0028	92.33587665	24.32107537	10.85
962	369	515	-170.2168	518.5160	0.0023	0.0023	92.34033429	24.43659346	12.92
679	375	520	-185.3800	863.5363	0.0010	0.0012	92.34458229	24.34073948	11.43
963	386	529	-202.1027	562.2854	0.0013	0.0017	92.35001438	24.42440344	12.30
699	394	537	-221.5466	768.5136	0.0022	0.0023	92.35571507	24.36709816	12.53
983	396	539	-222.5051	628.9943	0.0008	0.0012	92.35616384	24.40585250	11.43
470	397	542	-227.2442	798.1468	0.0009	0.0009	92.35741919	24.35886086	12.29
957	401	547	-233.9595	719.9456	0.0007	0.0009	92.35955510	24.38057653	9.47
656	405	551	-246.3449	764.8312	0.0011	0.0012	92.36328125	24.36809551	11.66
590			-254.7560	975.3324	0.0025	0.0025	92.36560577	24.30961409	12.33
989	412		-273.2967	651.2125	0.0014	0.0016	92.37163129	24.39962806	13.35
913			-297.5941	596.5943	0.0010	0.0012	92.37910647	24.41477393	13.30
596	426	570	-306.3110	892.1581	0.0014	0.0016	92.38141761	24.33266363	11.46
935	428	571	-312.6481	681.4128	0.0008	0.0011	92.38359848	24.39119715	11.14
903			-329.8979	383.1516	0.0027	0.0026	92.38921601	24.47402845	11.44
480	433	579	-344.6161	912.8653	0.0018	0.0018	92.39307030	24.32687004	12.75
603	434	580	-345.4622	866.1558	0.0013	0.0012	92.39338439	24.33984399	10.63
862	449	598	-372.4204	576.6086	0.0009	0.0014	92.40195705	24.42024381	12.77
950	451	601	-378.3219	726.1392	0.0010	0.0013	92.40357401	24.37870106	11.19
489	454	603	-381.3933	805.0586	0.0011	0.0012	92.40441382	24.35677560	13.12
915	456	605	-391.6268	673.6241	0.0008	0.0011	92.40769643	24.39327362	13.48
719	457	606	-393.9079	919.1540	0.0023	0.0025	92.40808879	24.32506833	10.04
798			-406.7233	836.6876	0.0011	0.0012	92.41209795	24.34796119	12.22
900	468	619	-411.2715	535.2052	0.0010	0.0016	92.41386101	24.43170092	12.24
564	472	622	-429.6251	920.9994	0.0012	0.0015	92.41897443	24.32451506	11.73
859			-434.1128	407.8234	0.0029	0.0031	92.42099098	24.46705834	13.67
944			-464.7764	424.4672	0.0025	0.0025	92.43032751	24.46239945	13.05
659	481	633	-478.3271	739.3035	0.0014	0.0018	92.43405536	24.37492940	13.11
706	498	652	-545.9203	755.3201	0.0025	0.0027	92.45464705	24.37039920	13.75
797	502	656	-552.2129	793.5396	0.0017	0.0022	92.45651467	24.35977503	9.91
445	506	663	-605.0441	997.6470	0.0030	0.0038	92.47234325	24.30301297	13.57
457	507	664	-607.4605	740.4768	0.0012	0.0024	92.47343407	24.37444603	10.63
965			-888.9762	717.0597	0.0023	0.0063	92.55932109	24.38057188	13.18